

Supplementary Material

Second-harmonic generation responses in low-dimensional metal bromides functionalized with L-arginine

Juan Cheng, Yingjie Wang, Qinglan Zhong, Ziyu Zhou, Hongmei Zeng,* Guohong Zou and Zhien Lin*

College of Chemistry, Sichuan University, Chengdu 610064, China

* To whom correspondence should be addressed. E-mail: zenghongmei@scu.edu.cn (H. Zeng); zhienlin@scu.edu.cn (Z. Lin)

Synthesis

All of the starting reagents were used without further purification: L-arginine (98%), $\text{CdBr}_2 \cdot 4\text{H}_2\text{O}$ (AR 99%), PbBr_2 (AR 99%), and HBr (ACS 48%) were purchased from Shanghai Macklin Biochemical Co., Ltd and ZnBr_2 (AR 98%) were purchased from Aladdin Industrial Corporation.

$(\text{L-C}_6\text{H}_{15}\text{N}_4\text{O}_2)\text{ZnBr}_3$ (**1**) was prepared by mixing ZnBr_2 (0.113 g), L-arginine (0.087g), HBr (48%, 60 μL), and H_2O (1.5 mL) in a glass vial. The mixture was stirred for 10 min at room temperature. Colorless flake crystals were obtained after seven days by slow evaporation of the resulting solution at room temperature (98% yield based on zinc).

$(\text{L-C}_6\text{H}_{14}\text{N}_4\text{O}_2)_2\text{Cd}_2\text{Br}_4$ (**2**) was prepared by mixing $\text{CdBr}_2 \cdot 4\text{H}_2\text{O}$ (0.344 g), L-arginine (0.263 g), HBr (48%, 57 μL), and H_2O (1.5 mL) in a glass vial. The mixture was stirred for 10 min at room temperature. Colorless flake crystals were obtained after two days by slow evaporation of the resulting solution at room temperature (78% yield based on cadmium).

$(\text{L-C}_6\text{H}_{16}\text{N}_4\text{O})_2\text{Pb}_3\text{Br}_{10} \cdot 2\text{H}_2\text{O}$ (**3**) was prepared by mixing PbBr_2 (0.184g), L-arginine (0.087g), and HBr (48%, 2mL) in a glass vial. The mixture was stirred for 10 min at room temperature. Colorless block crystals were obtained by slow evaporation of the clear solution at 70 °C over a period of two days (53% yield based on lead).

Structural determination

Single crystal X-ray diffraction (XRD) data were collected on Bruker D8 Venture diffractometer at room temperature. The crystal structures were solved by direct methods. The structures were refined on F^2 by full-matrix least-squares methods using the *SHELXTL* program package.^{1,2}

Powder XRD Analysis

Powder XRD data were obtained using a Shimadzu XRD-6100 diffractometer with Cu-K α radiation ($\lambda = 1.5418 \text{ \AA}$), in the angular range of $2\theta = 5\text{--}50^\circ$, and with a scan step width of 0.02° and a fixed time of 0.2 s.

Thermal Stability Analysis

Thermogravimetric analysis (TGA) was conducted using a Shimadzu DTG-60H unit under an N₂ atmosphere, with a heating rate of $10 \text{ }^\circ\text{C min}^{-1}$ in the range of 30 to 800 $^\circ\text{C}$.

UV-Vis Diffuse Reflectance Spectroscopy

The UV–vis diffuse reflectance spectrum of the as-synthesized compounds were recorded at room temperature on a Shimadzu UV-2600 UV–vis spectrophotometer in the wavelength range of 200–800 nm. BaSO₄ powder was used as 100% reflectance reference. The Kubelka-Munk function^{3, 4} was used to calculate the absorption spectra from the reflection spectra: $F(R) = \alpha/S = (1-R)^2/2R$, where R is the reflectance, α is the absorption coefficient, and S is the scattering coefficient.

Second-Harmonic Generation Tests

The Kurtz and Perry method was used to measure powder second harmonic generation (SHG) signals at room temperature.⁵ The SHG efficiency mainly depends on the particle size, and the crystalline compound was ground and divided into the following particle sizes: 25–45, 45–58, 58–75, 75–106, 106–150 and 150–212 μm . Microcrystalline KH₂PO₄ (KDP) with the same particle size was used as a reference. The measurements were performed using Q-switched Nd: YAG lasers with visible light at 1064 nm, and a cut-off filter was used to limit the background flash light on the sample, and the SHG signal is recorded by a photomultiplier tube.

Computational Methods

In order to understand the relationship between structure and properties of compound **3**,

the first-principles calculations were carried out by using the CASTEP software package.⁶ The band structure, density of states (DOS) / partial density of states (PDOS), and optical properties of compound **3** were calculated. The generalized gradient approximation (GGA) with Perdew–Burke–Ernzerhof (PBE) was used for all the calculations.⁷ All the atoms were performed by Norm-conserving pseudopotentials (NCP), with H 1s¹, C 2s²2p², N 2s²2p³, O 2s²2p⁴, Br 4s²4p⁵, Pb 5d¹⁰6s²6p² treated as valence electrons.⁸ The criteria of convergences of energy are set to 1.0e-6 eV/atom. The kinetic energy cutoff of 820 eV and the k-point sampling of 4 × 3 × 3 were chosen for the compound **3**.⁹ All other parameter settings are CASTEP default values.

To obtain the linear optical properties, the complex dielectric function $\varepsilon(\omega) = \varepsilon_1(\omega) + i\varepsilon_2(\omega)$ has been determined in the random phase approximation from the PBE wavefunctions. The imaginary part of the dielectric function due to direct inter-band transitions is given by the expression,

$$\varepsilon_2(\hbar\omega) = \frac{2e^2\pi}{\Omega\varepsilon_0} \sum_{k,v,c} \left| \langle \psi_k^c | u \cdot r | \psi_k^v \rangle \right|^2 \delta(E_k^c - E_k^v - E) \quad (\text{equation S1})$$

where Ω , ω , u , v and c are the unit-cell volume, photon frequencies, the vector defining the polarization of the incident electric field, valence and conduction bands, respectively. The real part of the dielectric function is obtained from ε_2 by a Kramers-Kronig transformation,

$$\varepsilon_1(\omega) = 1 + \left(\frac{2}{\pi}\right) \int_0^{+\infty} d\omega' \frac{\omega'^2 \varepsilon_2(\omega')}{\omega'^2 - \omega^2} \quad (\text{equation S2})$$

In calculation of the static $\chi^{(2)}$ coefficients, the so-called length-gauge formalism derived by Aversa and Sipe¹⁰ and modified by Rashkeev *et al*¹¹ is adopted, which has been proved to be successful in calculating the second order susceptibility for semiconductors

and insulators.^{12, 13} In the static case, the imaginary part of the static second-order optical susceptibility can be expressed as:

$$\begin{aligned}
& \chi^{abc} \\
&= \frac{e^3}{\hbar^2 \Omega} \sum_{nml,k} \frac{r_{nm}^a (r_{ml}^b r_{ln}^c + r_{ml}^c r_{ln}^b)}{2\omega_{nm} \omega_{ml} \omega_{ln}} [\omega_n f_{ml} + \omega_m f_{ln} + \omega_l f_{nm}] \\
&+ \frac{ie^3}{4\hbar^2 \Omega} \sum_{nm,k} \frac{f_{nm}}{\omega_{mn}^2} [r_{nm}^a (r_{mn;c}^b + r_{mn;b}^c) + r_{nm}^b (r_{mn;c}^a + r_{mn;a}^c) + r_{nm}^c (r_{mn;b}^a + r_{mn;a}^b)]
\end{aligned} \tag{equation S3}$$

where r is the position operator, $\hbar\omega_{nm} = \hbar\omega_n - \hbar\omega_m$ is the energy difference for the bands m and n , $f_{mn} = f_m - f_n$ is the difference of the Fermi distribution functions, subscripts a , b , and c are Cartesian indices, and $r_{mn;a}^b$ is the so-called generalized derivative of the coordinate operator in k space,

$$r_{nm;a}^b = \frac{r_{nm}^a \Delta_{mn}^b + r_{nm}^b \Delta_{mn}^a}{\omega_{nm}} + \frac{i}{\omega_{nm}} \times \sum_l (\omega_{lm} r_{nl}^a r_{lm}^b - \omega_{nl} r_{nl}^b r_{lm}^a) \tag{equation S4}$$

where $\Delta_{nm}^a = (p_{nn}^a - p_{mm}^a) / m$ is the difference between the electronic velocities at the bands n and m .

Table S1 Select hydrogen bonds for compound **1**.

D–H···A	D–H (Å)	H···A (Å)	D···A (Å)	<(DHA) (°)
N(1)–H(1A)···Br(1) ¹	0.89	2.79	3.498(7)	137.0
N(1)–H(1A)···Br(2) ¹	0.89	2.93	3.638(7)	137.2
N(1)–H(1B)···Br(1) ²	0.89	2.86	3.573(7)	137.7
N(1)–H(1B)···Br(2) ³	0.89	2.83	3.378(6)	121.0
N(1)–H(1C)···O(1) ³	0.89	2.07	2.913(9)	157.6
N(2)–H(2)···Br(3) ⁴	0.86	3.13	3.623(8)	118.4
N(3)–H(3A)···Br(2) ⁵	0.86	3.07	3.626(8)	124.8
N(3)–H(3A)···Br(3) ⁵	0.86	2.88	3.666(9)	153.3
N(3)–H(3B)···Br(1) ⁴	0.86	2.65	3.460(8)	158.3
N(4)–H(4A)···O(2) ²	0.86	2.30	2.961(10)	133.5
N(4)–H(4B)···Br(3) ⁵	0.86	2.83	3.623(9)	155

Symmetry transformations used to generate equivalent atoms:
¹1+X, +Y, +Z; ²1-X, -1/2+Y, 1/2-Z; ³1-X, 1/2+Y, 1/2-Z; ⁴1/2-X, 1-Y, 1/2+Z; ⁵1/2-X, -Y, 1/2+Z.

Table S2. Selected bond lengths (Å) for compound **1**

Br1–Zn1	2.4166(15)	N2–C7	1.311(13)
Br2–Zn1	2.3990(13)	N3–C7	1.320(11)
Br3–Zn1	2.3741(15)	N4–C7	1.308(12)
Zn1–O1	1.990(6)	C1–C2	1.525(10)
O1–C1	1.263(9)	C2–C3	1.525(10)
O2–C1	1.232(10)	C3–C4	1.529(11)
N1–C2	1.493(10)	C4–C5	1.509(11)
N2–C5	1.459(10)		

Table S3. Selected bond lengths (Å) for compound **2**

Cd1–Br1	2.574(2)	N2–C6	1.33(2)
Cd1–Br2	2.605(2)	N3–C6	1.33(2)
Cd1–O1	2.369(13)	N4–C6	1.33(3)
Cd1–O3	2.291(13)	N5–C8	1.48(2)
Cd1–N1	2.315(13)	N6–C11	1.46(2)
Cd2–Br3	2.596(2)	N6–C12	1.31(2)
Cd2–Br4	2.586(2)	N7–C12	1.32(2)
Cd2–O1	2.265(12)	N8–C12	1.34(2)
Cd2–O3	2.367(13)	C1–C2	1.56(2)
Cd2–N5	2.316(16)	C2–C3	1.51(2)
O1–C1	1.27(2)	C3–C4	1.53(3)
O2–C1	1.22(2)	C4–C5	1.47(3)
O3–C7	1.26(2)	C7–C8	1.54(2)
O4–C7	1.21(2)	C8–C9	1.52(2)
N1–C2	1.46(2)	C9–C10	1.54(2)
N2–C5	1.48(2)	C10–C11	1.49(3)

Table S4. Selected bond lengths (Å) for compound **3**

Pb1–Br1	2.875(3)	N2–C5	1.45(4)
Pb1–Br2	2.809(3)	N2–C6	1.30(3)
Pb1–Br3	3.014(4)	N3–C6	1.35(4)
Pb1–Br4	3.223(3)	N4–C6	1.35(4)
Pb1–Br6 ¹	3.087(3)	C1–C2	1.52(3)
Pb2–Br3	3.063(4)	C2–C3	1.52(3)
Pb2–Br4	3.052(4)	C3–C4	1.53(3)
Pb2–Br5	3.052(4)	C4–C5	1.56(3)
Pb2–Br6	2.903(3)	O3–C7	1.21(3)
Pb2–Br7	2.992(3)	O4–C7	1.39(3)
Pb2–Br8 ¹	3.098(3)	N5–C8	1.40(3)
Pb3–Br5	3.174(3)	N6–C11	1.44(3)
Pb3–Br7	2.984(4)	N6–C12	1.31(3)
Pb3–Br8	3.085(4)	N7–C12	1.35(3)
Pb3–Br9	2.827(3)	N8–C12	1.27(3)
Pb3–Br10	2.904(3)	C7–C8	1.44(3)
O1–C1	1.27(3)	C8–C9	1.62(3)
O2–C1	1.18(3)	C9–C10	1.52(3)
N1–C2	1.49(3)	C10–C11	1.49(3)

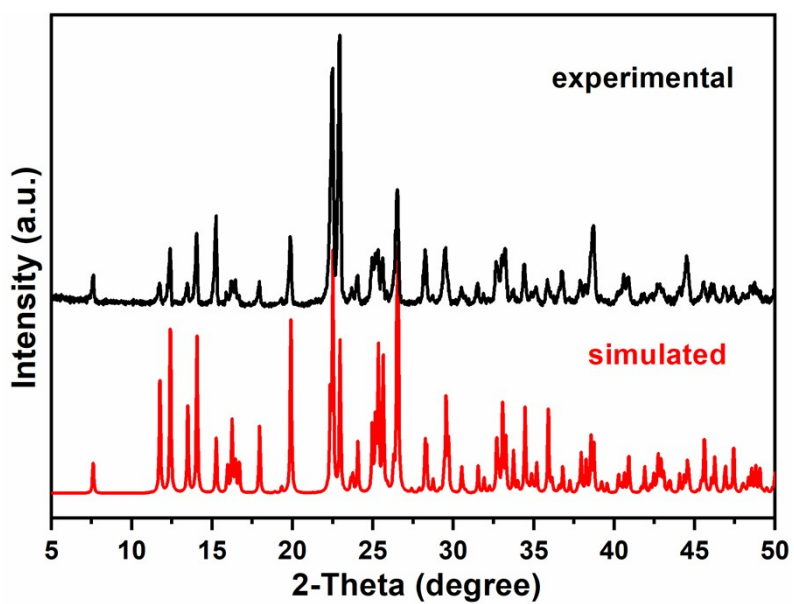


Figure S1. Simulated and experimental powder XRD patterns for compound 1.

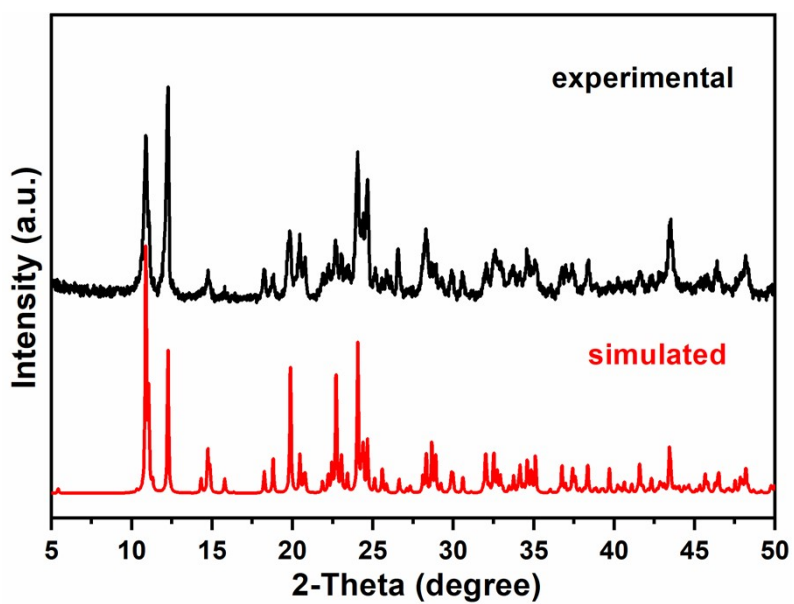


Figure S2. Simulated and experimental powder XRD patterns for compound 2.

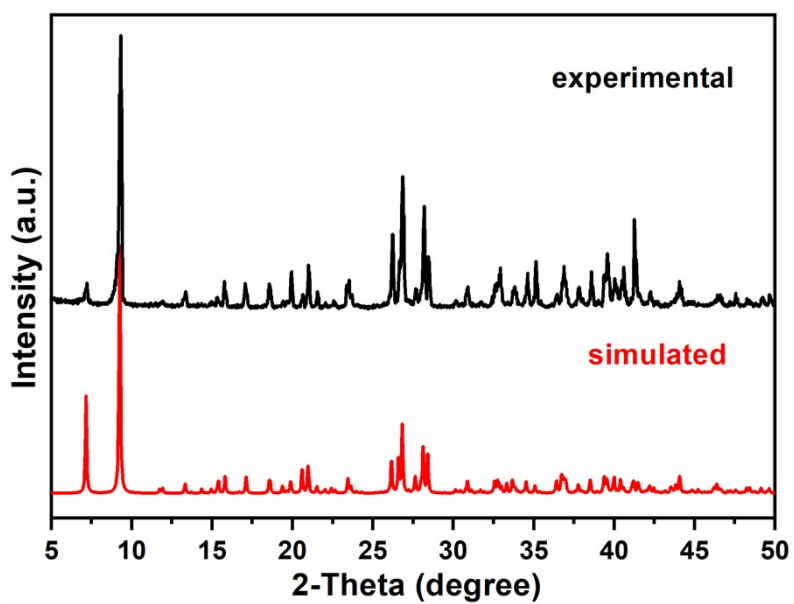


Figure S3. Simulated and experimental powder XRD patterns for compound 3.

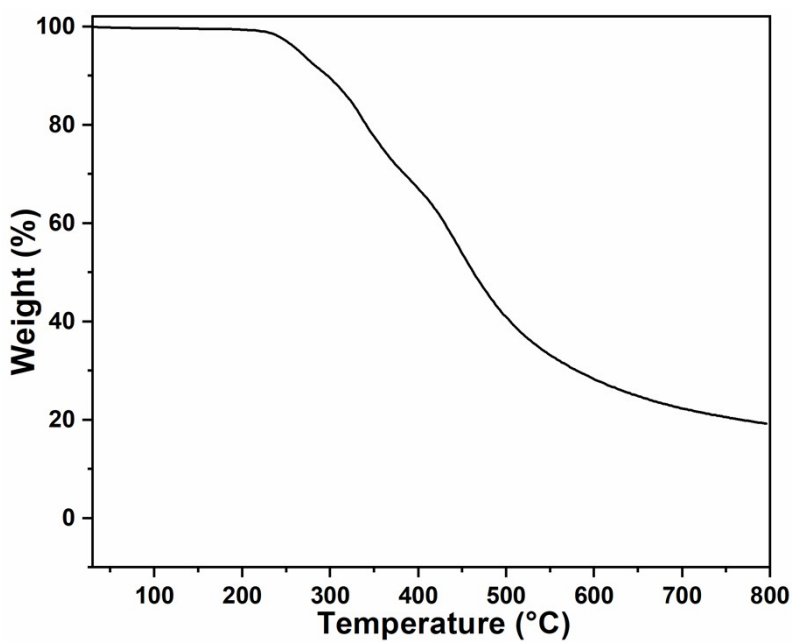


Figure S4. TGA curve of compound 1.

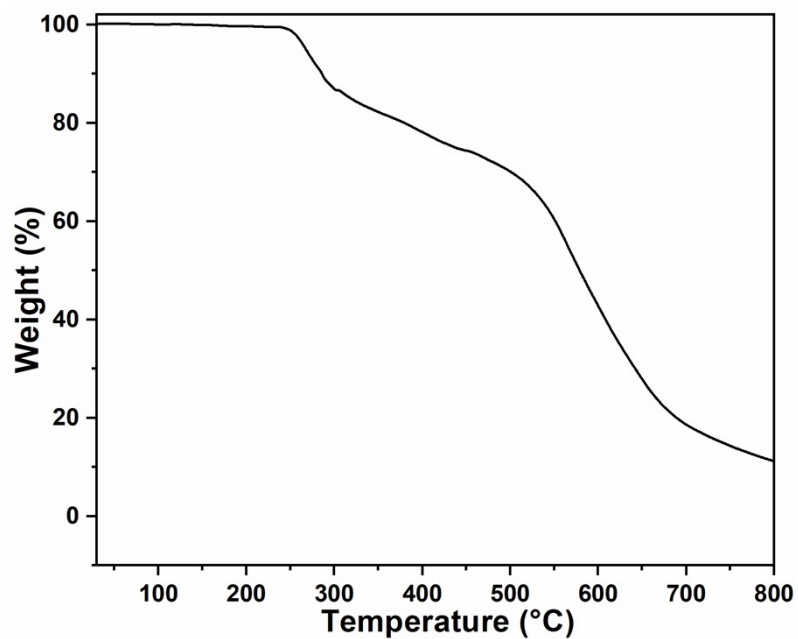


Figure S5. TGA curve of compound 2.

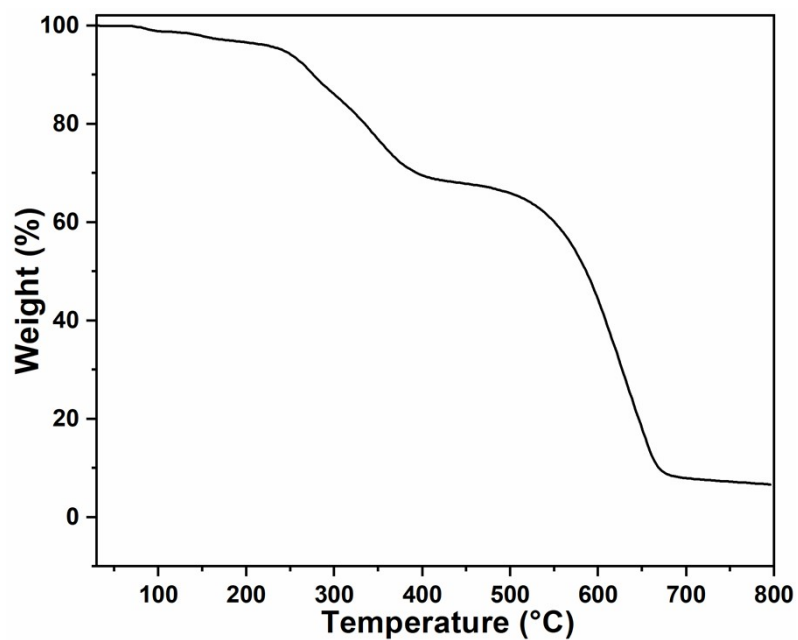


Figure S6. TGA curve of compound 3.

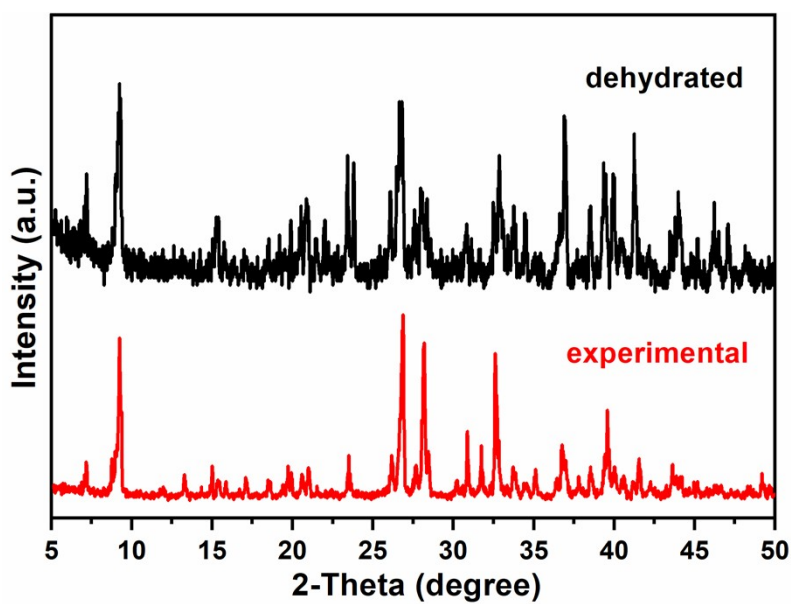


Figure S7. Experimental and dehydrated powder XRD patterns for compound 3.

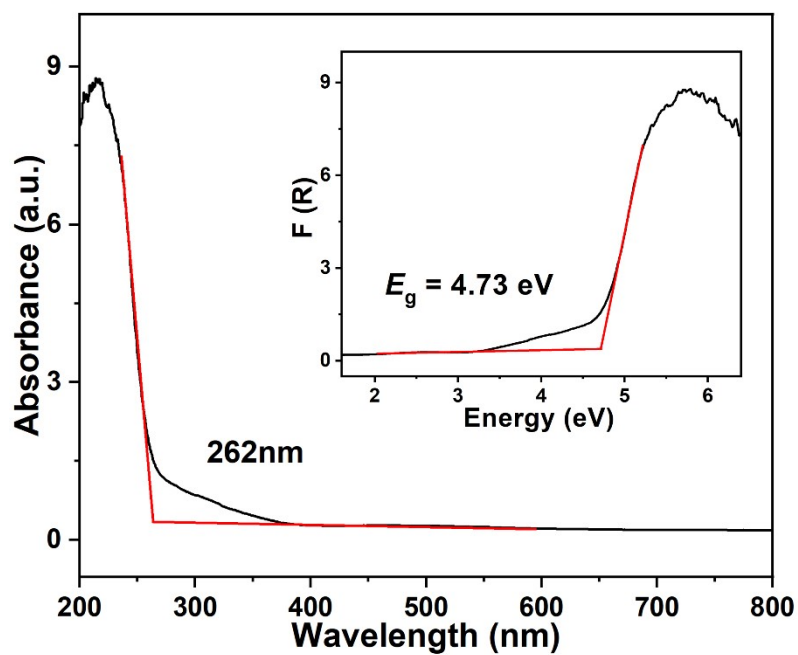


Figure S8. The UV/vis absorption spectrum of compound 1. The inset shows the bandgap of compound 1.

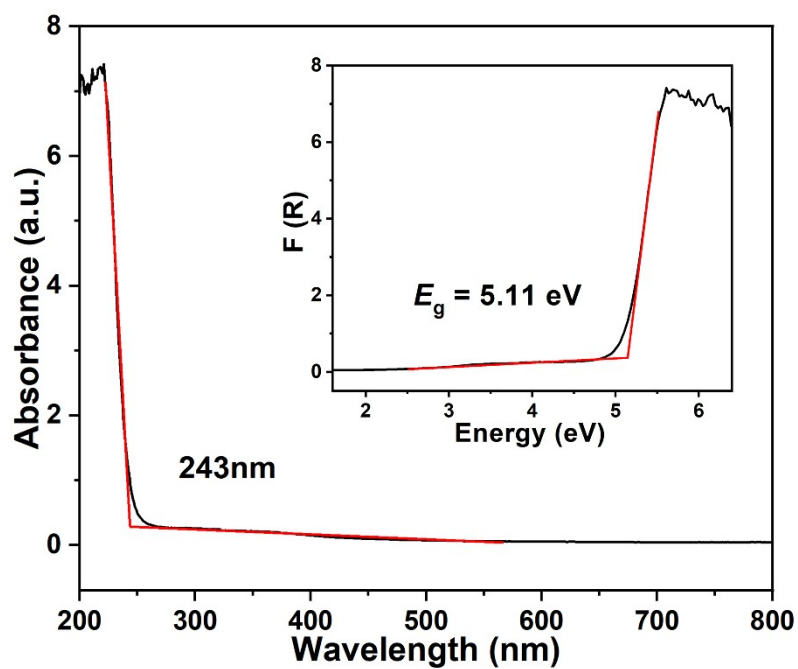


Figure S9. The UV/vis absorption spectrum of compound **2**. The inset shows the bandgap of compound **2**.

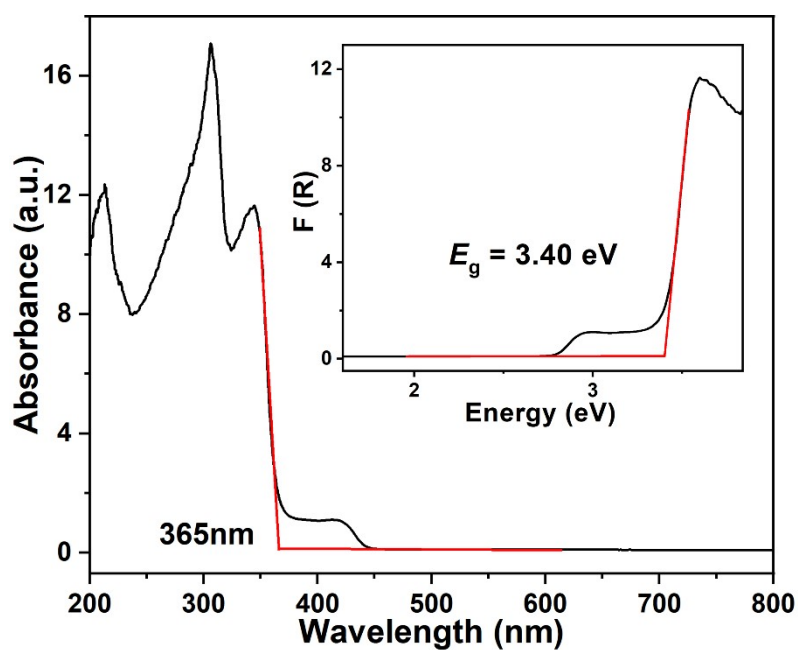


Figure S10. The UV/vis absorption spectrum of compound **3**. The inset shows the bandgap of compound **3**.

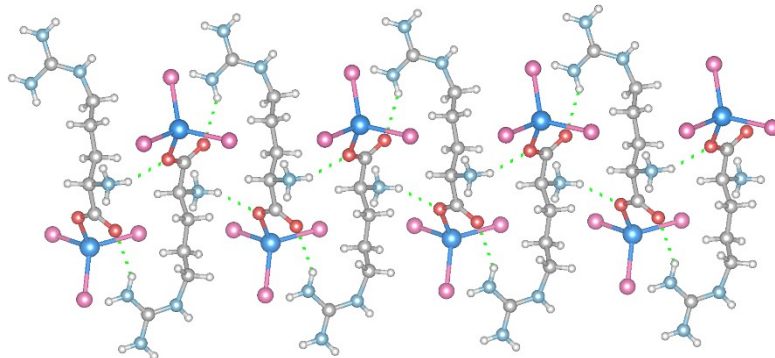


Figure S11. Hydrogen bonds in compound 1.

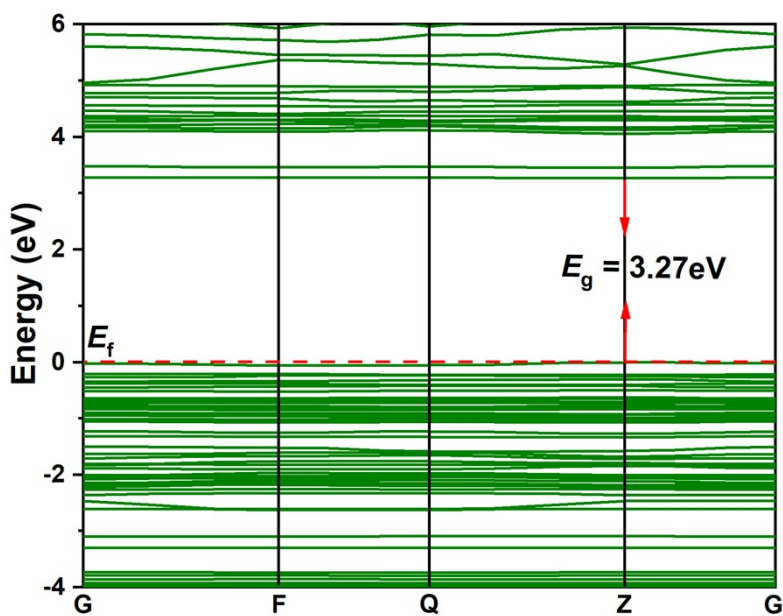


Figure S12. Calculated band structure of compound 3 (the Fermi level is set at 0 eV)..

References

- (1) G. M. Sheldrick, *Acta Crystallogr. Sect. A*, 2015, **71**, 3.
- (2) G. M. Sheldrick, *Acta Crystallogr. Sect. A*, 2008, **64**, 112.
- (3) P. Kubelka.; F. Munk, *Z. Technol. Phys.* 1931, **12**, 593.
- (4) J. Tauc, *Mater. Res. Bull.* 1970, **5**, 721.
- (5) S. K. Kurtz.; T. T. Perry, *J. Appl. Phys.* 1968, **39**, 3798.
- (6) M. D. Segall.; P. J. D. Lindan.; M. J. Probert.; C. J. Pickard.; P. J. Hasnip.; S. J. Clark.; M. C. Payne, *J. Phys. Condens. Matter* 2002, **14**, 2717.
- (7) J. P. Perdew.; K. Burke.; M. Ernzerhof, *Phys. Rev. Lett.* 1996, **77**, 3865.
- (8) K. Kobayashi, *Comput. Mater. Sci.* 1999, **14**, 72.
- (9) D. Vanderbilt, *Phys. Rev. B* 1990, **41**, 7892.
- (10) G. Kresse, VASP, 5.3.5; <http://cms.mpi.univie.ac.at/vasp/vasp/vasp.html>. 2014.
- (11) S. N. Rashkeev.; W. R. L. Lambrecht.; B. Segall, *Phys. Rev. B* 1998, **57**, 3905.
- (12) B. Champagne.; D. M. Bishop, *Adv. Chem. Phys.* 2003, **126**, 41.
- (13) A. H. Reshak.; S. Auluck.; I. V. Kityk, *Phys. Rev. B: Condens. Matter Mater. Phys.* 2007, **75**, 245120.